Blocking the mitochondrial apoptotic pathway preserves motor neuron viability and function in a mouse model of amyotrophic lateral sclerosis

Nichole A. Reyes, … , Eric J. Huang, Scott A. Oakes

Research Article **Neuroscience**

Apoptosis of motor neurons is a well-documented feature in amyotrophic lateral sclerosis (ALS) and related motor neuron diseases (MNDs). However, the role of apoptosis in the pathogenesis of these diseases remains unresolved. One possibility is that the affected motor neurons only succumb to apoptosis once they have exhausted functional capacity. If true, blocking apoptosis should confer no therapeutic benefit. To directly investigate this idea, we tested whether tissue-specific deletion in the mouse CNS of BCL2-associated X protein (BAX) and BCL2-homologous antagonist/killer (BAK), 2 proapoptotic BCL-2 family proteins that together represent an essential gateway to the mitochondrial apoptotic pathway, would protect against motor neuron degeneration. We found that neuronal deletion of *Bax* and *Bak* in a mouse model of familial ALS not only halted neuronal loss, but prevented axonal degeneration, symptom onset, weight loss, and paralysis and extended survival. These results show that motor neurons damaged in ALS activate the mitochondrial apoptotic pathway early in the disease process and that apoptotic signaling directly contributes to neuromuscular degeneration and neuronal dysfunction. Hence, inhibiting apoptosis upstream of mitochondrial permeabilization represents a possible therapeutic strategy for preserving functional motor neurons in ALS and other MNDs.

Find the latest version:

https://jci.me/42986/pdf

Blocking the mitochondrial apoptotic pathway preserves motor neuron viability and function in a mouse model of amyotrophic lateral sclerosis

Nichole A. Reyes,[1] Jill K. Fisher,[2] Kathryn Austgen,[1] Scott VandenBerg,[3] Eric J. Huang,[1,4] and Scott A. Oakes[1]

[1]Department of Pathology, University of California, San Francisco, San Francisco, California, USA. [2]Department of Pathology, Harvard Medical School, Dana-Farber Cancer Institute, Boston, Massachusetts, USA. [3]Department of Pathology, University of California, San Diego, La Jolla, California, USA. [4]Pathology Service, Veterans Affairs Medical Center, San Francisco, California, USA.

Apoptosis of motor neurons is a well-documented feature in amyotrophic lateral sclerosis (ALS) and related motor neuron diseases (MNDs). However, the role of apoptosis in the pathogenesis of these diseases remains unresolved. One possibility is that the affected motor neurons only succumb to apoptosis once they have exhausted functional capacity. If true, blocking apoptosis should confer no therapeutic benefit. To directly investigate this idea, we tested whether tissue-specific deletion in the mouse CNS of BCL2-associated X protein (BAX) and BCL2-homologous antagonist/killer (BAK), 2 proapoptotic BCL-2 family proteins that together represent an essential gateway to the mitochondrial apoptotic pathway, would protect against motor neuron degeneration. We found that neuronal deletion of *Bax* and *Bak* in a mouse model of familial ALS not only halted neuronal loss, but prevented axonal degeneration, symptom onset, weight loss, and paralysis and extended survival. These results show that motor neurons damaged in ALS activate the mitochondrial apoptotic pathway early in the disease process and that apoptotic signaling directly contributes to neuromuscular degeneration and neuronal dysfunction. Hence, inhibiting apoptosis upstream of mitochondrial permeabilization represents a possible therapeutic strategy for preserving functional motor neurons in ALS and other MNDs.

Introduction

Neuronal tissues are susceptible to a number of insults that contribute to motor neuron dysfunction and cell death, including misfolded proteins, reactive oxygen and nitrogen species, calcium entry, excitotoxicity, trophic factor withdrawal, death receptor activation, and mitochondrial complex inhibition (1, 2). There is abundant evidence that injured motor neurons undergo apoptosis in a variety of motor neuron diseases (MNDs). For example, mouse models, cell culture systems, and/or postmortem tissues from affected patients of spinal muscular atrophy, Kennedy disease, and amyotrophic lateral sclerosis (ALS) show caspase activation in degenerating neurons (3–5). Caspase-3, one of the major cysteine-aspartate proteases responsible for degrading cellular components during apoptosis, is activated in both motor neurons and astrocytes contemporaneously with the first stages of motor neuron degeneration in the best-studied mouse models of ALS (6, 7). Moreover, inhibiting caspases through various approaches modestly improves outcome in several models of neurodegeneration (8–10). These findings suggest that apoptosis may actively contribute to the ongoing disease process.

In opposition to this view, recent temporal studies of neurodegenerative models have strongly argued that apoptosis is a relatively late event, preceded by earlier functional abnormalities (e.g., activation of cellular stress pathways, electrophysiological deficits) and microanatomical deficits (e.g., synapse loss, neurite retrac-

tion) (11–13). These studies have led to the widely held view that degenerating neurons activate apoptosis only after end-stage irreversible damage and functional exhaustion have already ensued. Therefore, the contribution of apoptosis to the pathology and/or clinical manifestations of neurodegeneration remains unresolved. Given the morbidity and mortality associated of these diseases and the current lack of effective therapies, it is essential to determine whether disruption of the apoptotic program represents a valid therapeutic strategy to treat MNDs such as ALS.

Results

To study the effects of disabling the mitochondrial (intrinsic) apoptotic pathway on the onset and progression of neurodegeneration in a mouse model of familial ALS, we generated mice deficient for BCL2-associated X protein (*Bax*) and BCL2-homologous antagonist/killer (*Bak*) in the CNS. In response to diverse types of cell injury, the proapoptotic BCL-2 proteins BAX and/or BAK homo-oligomerize at the outer mitochondrial membrane, which leads to efflux of proapoptotic mitochondrial matrix proteins (i.e., cytochrome *c*, SMAC/DIABLO) and activation of downstream effector caspases (i.e., caspase-3) (14–17). Cells doubly deficient in *Bax* and *Bak* are strikingly resistant to apoptosis in response to a wide range of intrinsic death stimuli (e.g., DNA damage, protein misfolding, reactive oxygen species). Since germline-deficient *Bax*−/−*Bak*−/− mice generally die in utero by embryonic day 18, we used mice with a previously described floxed (f) conditional allele of *Bax* and germline deletion of *Bak* (18). These *Bax*f/f*Bak*−/− mice were then bred to express *Cre* recombinase under the rat nestin
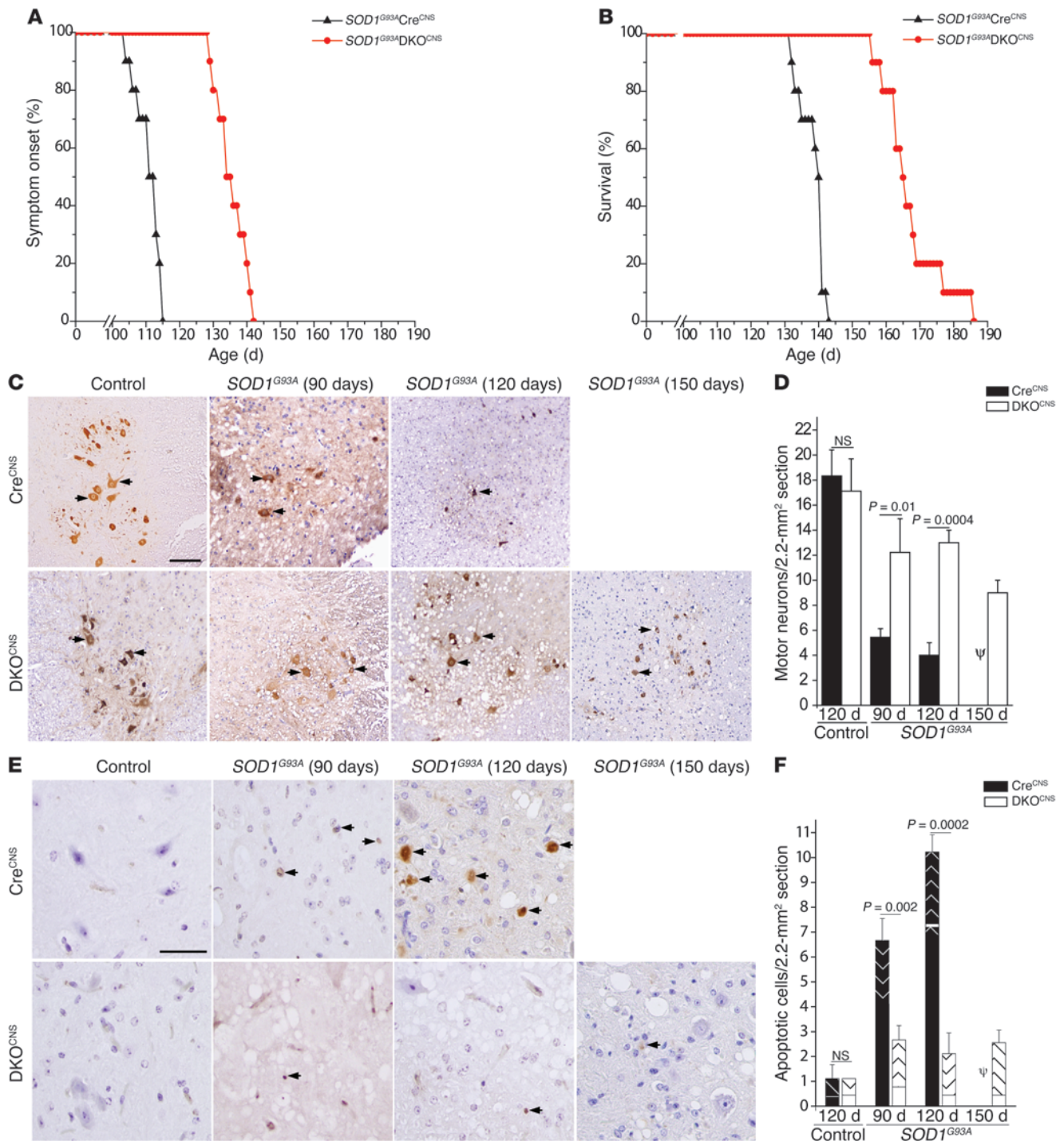
Figure 1
Deletion of BAX/BAK-dependent apoptosis delays symptom onset, prolongs survival, and preserves motor neurons in a mouse model of ALS. (**C** and **E**) Control mice were harvested at 120 days of age. Symptom onset occurred at 90 days and 120 days for *SOD1^{G93A}*Cre^{CNS} and *SOD1^{G93A}*DKO^{CNS} mice, respectively. End-stage occurred at 120 days and 150 days for *SOD1^{G93A}*Cre^{CNS} and *SOD1^{G93A}*DKO^{CNS} mice, respectively. (**A**) Symptom onset of *SOD1^{G93A}*Cre^{CNS} mice (111.3 ± 4.3 days) and *SOD1^{G93A}*DKO^{CNS} mice (135.6 ± 4.6 days). *P* < 0.0001, unpaired 2-tailed Student's *t* test. *n* = 10. (**B**) Survival of *SOD1^{G93A}*Cre^{CNS} mice (138.6 ± 3.8 days) and *SOD1^{G93A}*DKO^{CNS} mice (167.2 ± 8.7 days). *P* < 0.0001, log-rank test. *n* = 10. (**C**) Representative choline acetyltransferase staining (brown) of the anterior horn region of spinal cords from the indicated genotypes. Arrowheads indicate motor neurons. Scale bar: 200 μm. (**D**) Quantitation of anterior horn motor neurons from control and *SOD1^{G93A}* mice using choline acetyltransferase staining. (**E**) Representative spinal cord anterior horn sections stained with antibody to caspase-3 (brown). Arrowheads indicate activated caspase-3 staining. Scale bar: 100 μm. (**F**) Numbers of apoptotic cells (positive for activated caspase-3) from control and *SOD1^{G93A}* mice. The solid colors represent motor neurons, while the hatched pattern represents all other cell types. Quantification of data was analyzed via unpaired 2-tailed Student's *t* test (for all quantitation data, *n* = 3). ψ indicates that all mice were deceased at the indicated time point.
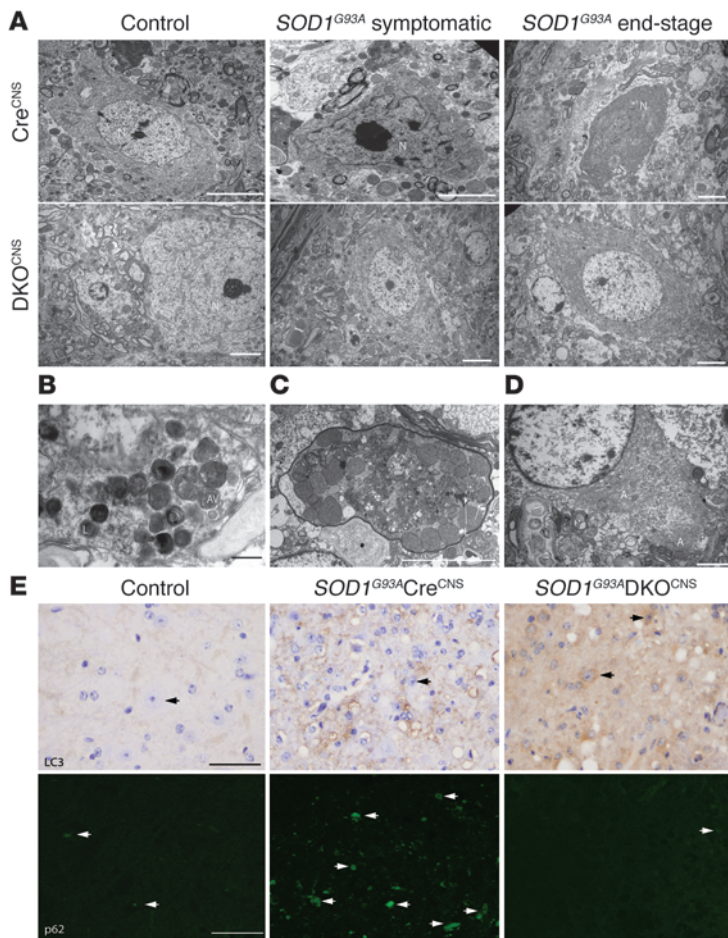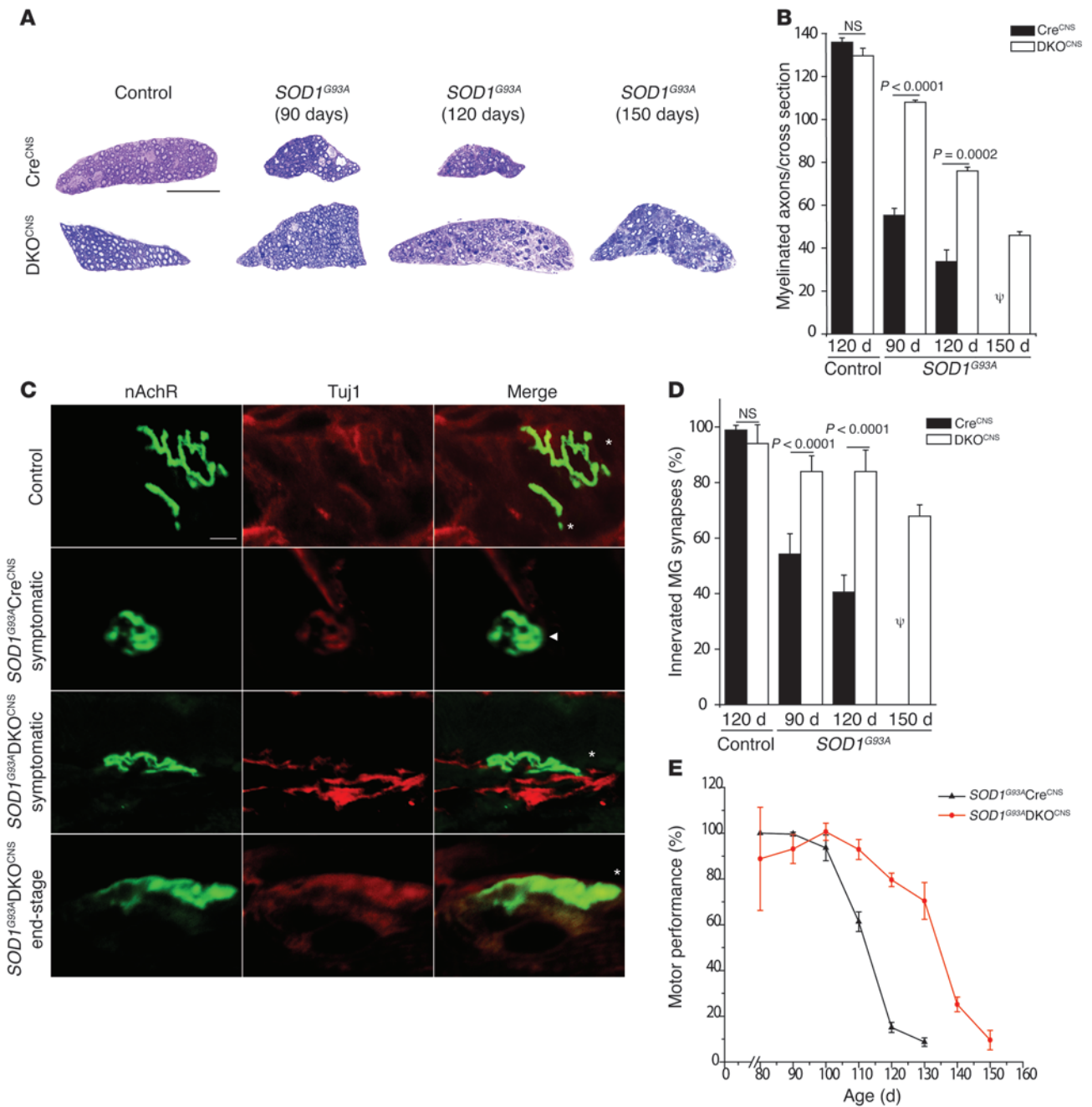
Figure 2
*SOD1[G93A]*DKO[CNS] neurons lack morphological features of apoptosis but show evidence of autophagy. (**A**–**D**) Transmission electron microscope images of motor neurons from control and *SOD1[G93A]* mice. (**A** and **E**) Control mice were harvested at 120 days. Symptom onset [symptomatic] began at 90 days and 120 days for *SOD1[G93A]*Cre[CNS] and *SOD1[G93A]*DKO[CNS] mice, respectively. End-stage began at 120 days and 150 days for *SOD1[G93A]*Cre[CNS] and *SOD1[G93A]*DKO[CNS] mice, respectively. (**B**–**D**) The *SOD1[G93A]*DKO[CNS] animal was harvested at end-stage (156 days). (**A**) Motor neurons from *SOD1[G93A]*Cre[CNS] animals appear apoptotic, while motor neurons from *SOD1[G93A]*DKO[CNS] animals appear healthy. Scale bars: 5 μm. (**B**) *SOD1[G93A]*DKO[CNS] motor neurons display morphological features of autophagy. Scale bar: 0.5 μm. (**C**) *SOD1[G93A]*DKO[CNS] motor axons are dystrophic and contain lysosomes. Scale bar: 5 μm. (**D**) Increased intracellular aggregates in *SOD1[G93A]*DKO[CNS] motor neurons. Scale bar: 2 μm. (**E**) Representative LC3 (brown) and p62 (green) staining of the anterior horn region of spinal cords from control and *SOD1[G93A]* mice. Arrows indicate motor neurons (top row) and positive p62 staining (bottom row). Scale bar: 100 μm (top row); 50 μm (bottom row). A, aggregates; AV, autophagic vesicle; L, lysosome; M, mitochondria; N, nucleus.

promoter (Nes*Cre*) to specifically delete *Bax* in the CNS (19). We confirmed *Cre*-mediated excision of *Bax* in the spinal cord by quantitative reverse-transcription PCR (RT-PCR) and immunoblotting (Supplemental Figure 1; supplemental material available online with this article; doi:10.1172/JCI42986DS1). These results indicated that *Bax[f/f]* is efficiently deleted from the CNS. The conditionally deficient *Bax* and *Bak* mice (DKO[CNS] mice) were born according to normal Mendelian ratios and showed no gross developmental

defects into adulthood (data not shown). Moreover, motor neuron numbers in DKO[CNS] mice were essentially identical to those of mice expressing Nes*Cre* alone and similar to those published in previous studies (ref. 20, Figure 1, C and D, and Supplemental Figure 5). Hence, this is an ideal genetic model to study motor neuron degeneration in the absence of BAX/BAK-dependent apoptosis.

We bred the DKO[CNS] mice to a model of familial ALS that expresses a toxic gain-of-function mutation in copper/zinc superoxide dismutase-1 (SOD1). Mice that express the human mutant *SOD1[G93A]*-transgene under the control of its endogenous promoter begin developing apoptosis of spinal cord motor neurons and paralysis of the hind limbs at approximately 100 days of age and become terminally paralyzed over the next approximately 30 days (21). We followed ALS onset and survival in *SOD1[G93A]* hemizygous mice on a BAX/BAK-positive versus DKO[CNS] background. *Bax* and/or *Bak* heterozygosity failed to affect symptom onset or survival (Supplemental Figure 2 and ref. 22); therefore, we pooled results from mice expressing at least one allele of both *Bax* and *Bak* into a single littermate cohort (Cre[CNS] mice). To minimize differences due to environment and gender, we compared identically housed, congenic cohorts with an equal number of males and females. Weight loss is an accepted measurement of symptom onset (motor dysfunction) and progression in this model of neurodegeneration (20, 23). Symptom onset was significantly delayed by approximately 3.5 weeks in the *SOD1[G93A]*DKO[CNS] mice as compared with that of the *SOD1[G93A]*Cre[CNS] mice (Figure 1A). Moreover, the *SOD1[G93A]*DKO[CNS] mice lived almost 1 month longer than *SOD1[G93A]*Cre[CNS] mice (167.2 and 138.6 days, respectively; *P* < 0.0001), representing an approximately 21% extension in life span (Figure 1B). In agreement with prior reports, gender did not result in a statistically significant difference in symptom onset or survival (Supplemental Figure 3 and ref. 24). Notably, at the age when the *SOD1[G93A]*Cre[CNS] mice were terminally paralyzed, the majority of the *SOD1[G93A]*DKO[CNS] mice showed no weight loss or paralysis. Interestingly, *SOD1[G93A]* mice, deficient in either *Bax* (Bax[CNS]) or *Bak*, also outlived *SOD1[G93A]*Cre[CNS] littermates, albeit to a lesser degree than the *SOD1[G93A]*DKO[CNS] mice (Supplemental Figure 4), suggesting a gene-dosage effect. The significant delay in symptom onset and extended survival of the DKO[CNS] ALS mice strongly suggest that the mitochondrial apoptotic pathway directly contributes to pathogenesis in this model of neurodegeneration.

Delayed paralysis and extended life span were associated with conspicuous preservation of motor neurons in the *SOD1[G93A]*DKO[CNS] mice that continued even through end-stage paralysis (Figure 1, C and D, via choline acetyltransferase staining and Supplemental Figure 5 via cresyl violet staining). As such, it took the *SOD1[G93A]*DKO[CNS] mice 150 days to approach the same degree of motor neuron loss seen in the *SOD1[G93A]*Cre[CNS] littermates at 90 days of age. Motor neuron survival in the *SOD1[G93A]*DKO[CNS] mice strongly correlated with decreased apoptosis, as determined by caspase-3 activation and TUNEL staining (Figure 1, E and F, and Supplemental Figure 6). This is striking in comparison with the *SOD1[G93A]*Cre[CNS] cohort, which showed caspase-3 activation and TUNEL staining as early as

Figure 3
Deletion of BAX/BAK preserves neuronal function. (**A** and **C**) Control, symptomatic, and end-stage are as defined as in the legend for Figure 2. (**A**) Representative ventral root sections from control and *SOD1*^{G93A} mice stained with toluidine blue. Scale bar: 200 μm. (**B**) Quantitation of myelinated ventral root axons from control and *SOD1*^{G93A} mice. *n* = 3. (**C**) Representative neuromuscular junction images from control and *SOD1*^{G93A} mice stained with FITC-conjugated α-bungarotoxin (green) and antibody to Tuj1 (red). Asterisks and arrowheads indicate fully innervated and partially innervated neuromuscular junctions, respectively. Notice the rounded, degenerated appearance of the *SOD1*^{G93A}Cre^{CNS} symptomatic neuromuscular junction. nAchR, nicotinic acetylcholine receptor. Scale bar: 8 μm. (**D**) Percentage of innervated synapses in control and *SOD1*^{G93A} mice as quantified from neuromuscular junction staining. *n* = 2. (**E**) Percentage of the longest rotarod performance by each mouse (*n* = 3 for each group). *P* < 0.05 via ANOVA. (**B** and **E**) Data were analyzed using unpaired 2-tailed Student's *t* test. ψ indicates that all mice were deceased at the indicated time point.

Table 1

Summary of quantitation data in control and *SOD1^G93A^* mice

	Control (120 days)	*SOD1^G93A^* (90 days)	*SOD1^G93A^* (120 days)	*SOD1^G93A^* (150 days)
No. motor neurons/2.2-mm² section[A]				
Cre^CNS^	16.4 ± 4.8	8.5 ± 2.1	4.7 ± 0.3	0[B]
DKO^CNS^	17.1 ± 2.6	12 ± 1	11.6 ± 2.2	8.6 ± 0.7
No. apoptotic cells/2.2-mm² section				
Cre^CNS^	1.2 ± 0.5	7 ± 0.9	10.2 ± 0.5	0[B]
DKO^CNS^	1.3 ± 0.6	1 ± 0	2.7 ± 0.3	2.7 ± 0.3
No. myelinated axons/cross section				
Cre^CNS^	136 ± 2	56.7 ± 3.1	26.3 ± 0.6	0[B]
DKO^CNS^	128 ± 6.2	106.7 ± 2.1	76.1 ± 1.7	45.3 ± 1.5
Innervated MG synapses (%)				
Cre^CNS^	98.9 ± 1.7	54.2 ± 7.4	40.6 ± 6.1	0[B]
DKO^CNS^	94.1 ± 6.8	88 ± 4.7	84 ± 7.8	67.9 ± 4.1

Data were taken at the time indicated in each column head. [A]Via choline acetyltransferase staining. [B]All mice were deceased at the indicated time point. MG, medial gastrocnemii; %, percentage of innervated synapses.

90 days of age. These results indicate that activation of the mitochondrial apoptotic pathway is a critical route through which *SOD1^G93A^* triggers neuronal cell death early in the disease process.

In the absence of the mitochondrial apoptotic pathway, there is some eventual motor neuron loss in the *SOD1^G93A^*DKO^CNS^ mice, which is apparently independent of caspase-3 activation. These findings are consistent with the delayed cell death that eventually occurs in fibroblasts from *Bax^–/–^Bak^–/–^* mice when exposed to a range of intrinsic apoptotic stimuli (25).

To examine the morphological features of the diseased neurons, we performed EM on spinal cord sections from the ALS mice. While motor neurons from the *SOD1^G93A^*Cre^CNS^ mice showed morphological features of apoptosis as early as 90 days of age, many *SOD1^G93A^*DKO^CNS^ motor neurons lacked such features, even at end-stage disease (Figure 2A). With extended survival, the motor neurons from the *SOD1^G93A^*DKO^CNS^ mice showed increased intracellular aggregates, lysosomes, and autophagosomes (Figure 2, B–D). Moreover, spinal cord axons from the *SOD1^G93A^*DKO^CNS^ mice were dystrophic and contained prominent lysosomes at late stages of disease (Figure 2C), a hallmark of neuronal associated autophagy (26). To determine whether the increase in lysosomes and autophagosomes was due to the induction of autophagy, we stained spinal cord sections with LC3 (a marker of mature autophagosomes) (27) and p62 (a protein specifically degraded by autophagy) (28, 29). Interestingly, end-stage *SOD1^G93A^*DKO^CNS^ motor neurons showed accumulation of LC3 and diminished p62 staining, consistent with active autophagy (Figure 2E). This finding is consistent with the occurrence of autophagy in *Bax^–/–^Bak^–/–^* fibroblasts when challenged with various stresses (30). During disease progression, the *SOD1^G93A^*DKO^CNS^ motor neurons continued to accumulate SOD1-containing aggregates (Supplemental Figure 7). Thus, blocking the mitochondrial apoptotic pathway preserves motor neuron viability, despite amassing toxic protein species (31, 32).

To assess motor neuron function, we quantified the number of ventral root myelinated axons and innervated medial gastrocnemii synapses from the ALS mice. The *SOD1^G93A^*DKO^CNS^ mice retained significantly more myelinated axons and innervated synapses compared with those of the *SOD1^G93A^*Cre^CNS^ littermates (Figure 3, A–D), indicating functional preservation of spinal cord motor neurons. Furthermore, the neuromuscular junctions of *SOD1^G93A^*Cre^CNS^ mice were significantly more denervated and degenerated in comparison with those of age-matched *SOD1^G93A^*DKO^CNS^ mice (Figure 3, C and D). Finally, the *SOD1^G93A^*DKO^CNS^ mice maintained motor function, as measured by rotarod performance, significantly longer than *SOD1^G93A^*Cre^CNS^ littermates (Figure 3E). In accordance with a previous study on *Bax^–/–^* mice and rotarod performance (33), our DKO^CNS^ animals exhibit impaired performance on the rotarod at higher speeds, which likely explains the discrepancy found in protection against symptom onset data, between using weight loss (3.5 weeks) versus rotarod performance (1.5 weeks) as a measure of motor function. However, using either measurement, onset is significantly delayed in *SOD1^G93A^*DKO^CNS^ mice in comparison with *SOD1^G93A^*Cre^CNS^ littermates. Therefore, *SOD1^G93A^*DKO^CNS^ motor neurons not only demonstrate increased viability, but also retain functional capacity for an extended period of time after *SOD1^G93A^*Cre^CNS^ motor neurons succumb.

Discussion

In this study, we show that genetic deletion of the mitochondrial apoptotic pathway significantly preserves neuronal viability, motor function, and life span in a mouse model of familial ALS (see Table 1). Prior attempts have been made to partially address the role of apoptosis in the pathogenesis of neurodegeneration in mouse models of ALS. Neuron-specific overexpression of anti-apoptotic BCL-2 or administration of the broad-spectrum caspase inhibitor z-VADfmk extended life span by approximately 2 weeks in *SOD1^G93A^* mice (7, 34). Bcl-2 is less effective at blocking the mitochondrial apoptotic pathway than deletion of BAX/BAK and, when overexpressed, is known to regulate tangential cell death signals unrelated to the BAX/BAK pathway, such as calcium-induced death, autophagy, and cell cycle entry (35–38). Moreover, z-VADfmk is a potent inhibitor of several key downstream effector caspases that are activated only after BAX/BAK-dependent mitochondrial permeabilization has occurred, an event that is incompatible with long-term cell viability (39, 40). Finally, a role for BAX in this process was suggested when *SOD1^G93A^* mice bred to animals germline-deleted for *Bax* outlived *SOD1^G93A^* wild-type controls by about 2 weeks (22), in agreement with our results for *SOD1^G93A^* mice deficient for *Bax* in the CNS (*SOD1^G93A^Bax^–/–;CNS^* mice) (Supplemental Figure 4).

In contrast with our findings in the *SOD1^G93A^*DKO^CNS^ mice, Gould et al. reported no protection against neuromuscular denervation in the *SOD1^G93A^Bax^–/–^* mice (22) and therefore reasoned that targeting the intrinsic apoptotic pathway would provide little functional benefit against MNDs. However, BAX and BAK are often partly redundant in triggering apoptosis and must both be deleted for long-term protection from apoptotic stimuli in many cell types (14, 15). By conditionally deleting *Bax* and *Bak* specifically in the neurons of the ALS mouse, we show that the mitochondrial apoptotic pathway is a major contributor to the pathogenesis of this disease. Compared with the *SOD1^G93A^Bcl-2* and *SOD1^G93A^Bax^–/–^* mice (7, 34), the *SOD1^G93A^*DKO^CNS^ mice show an approximately 40% greater extension in survival. Moreover, the *SOD1^G93A^*DKO^CNS^ mice demonstrate a 1.33-fold and 3-fold increase in the preservation of innervated synapses at end-stage compared with the *SOD1^G93A^Bcl-2* and *SOD1^G93A^Bax^–/–^* animals,

respectively (22, 34). BAX/BAK deletion not only halts neuronal loss, but prevents axonal degeneration, symptom onset, weight loss, and paralysis and extends survival by approximately 21%. Hence, complete blockade of the mitochondrial apoptotic pathway through deletion of both BAX and BAK in ALS preserves neuronal function for an extended period. These findings suggest that the same mitochondrial apoptotic machinery first causes neuromuscular degeneration and neuronal dysfunction before ultimately triggering cell death.

Interestingly, blocking apoptosis also induced autophagy, a process implicated in the clearance of intracellular protein aggregates in several neurodegenerative diseases (41, 42). Mounting evidence supports the notion that autophagy plays a largely protective role in neurodegeneration (43–46). Indeed, a recent study reports that p62 interacts with mutant SOD1, suggesting a potential role for autophagy in the degradation of misfolded SOD1 species (47). However, further studies will need to be done to define the exact role of autophagy induction in ALS.

In summary, our findings show that the mitochondrial apoptotic pathway plays a direct role in the pathogenesis of familial ALS and suggest that inherited differences in the threshold for triggering apoptosis may be one determinant in susceptibility to disorders of motor neuron loss. As such, therapeutic interventions to inhibit apoptosis upstream of mitochondrial permeabilization represent a promising strategy to treat ALS and related MNDs (48).

Methods

Western blots and antibodies. Proteins from spinal cords were extracted in RIPA buffer (20 mM Tris-MOPS [pH 7.4], 150 mM NaCl, 1 mM EDTA, 1 mM EGTA, 1% NP-40) containing protease inhibitor cocktail (Roche). The extract was sonicated and then centrifuged at 15,682 g for 10 minutes at 4°C. Protein concentration was measured using BCA assay (Pierce). Sixty μg of each sample was loaded on a 10% Bis-Tris gel (Invitrogen), transferred to PVDF membranes, and immunoblotted with antibodies against BAX (1:1,000; Cell Signaling Technology), or actin (1:1,000; Chemicon). Horseradish peroxidase–conjugated secondary antibodies were purchased from Jackson ImmunoResearch Laboratories Inc. (anti-mouse and anti-rabbit antibodies) or Millipore. Membranes were developed with Western Lightning Chemiluminescence Reagent (PerkinElmer).

Quantitative RT-PCR and primers. Total RNA was extracted from spinal cords using the RNeasy Mini Kit (Qiagen). cDNA was generated using the SuperScript II Reverse Transcriptase Kit (Invitrogen). Bax transcript levels were assessed by using SYBR Green PCR Master Mix (Applied Biosystems) and were normalized to hypoxanthine phosphoribosyltransferase (HPRT) levels. Samples were run in triplicate. Primer sequences used for Bax were as follows: forward, 5′-GCTGACATGTTTGCTGATGG-3′; reverse, 5′-GAT-CAGCTCGGGCACTTTAG-3′.

Animal models. All animal experiments were performed in accordance with NIH guidelines and approved by the Institutional Animal Care and Use Committee at the University of California, San Francisco. The *Bax* conditionally deficient mice and *Bak*-null mice were a gift from O. Takeuchi (Immunology Frontier Research Center, Osaka University, Osaka, Japan) and the laboratory of the late Stanley J. Korsmeyer (Dana-Farber Cancer Center, Boston, Massachusetts, USA). The *Bax^flox^* mice were derived from injection of RW4 ES cells (strain 129/SvJ) into C57BL/6J recipients, and the resulting chimera were bred to C57BL/6J for germline transmission (18). *Bax^flox^* mice were backcrossed to C57BL/6J background for 6 generations prior to these experiments. *Bak^-/-^* mice were backcrossed to C57BL/6J background for 6 generations before breeding to *Bax^flox^* mice. Nes*Cre* (B6.Cg[SJL]-Tg[Nes-cre]1Kln/J) and *SOD1^G93A^* mice (B6SJL-Tg[SOD1-G93A]1Gur/J)

were purchased from The Jackson Laboratory and are on C57BL/6J background. Mice compared in this study were all littermates and housed together to minimize environmental factors. Mice were genotyped using PCR protocols from The Jackson Laboratory.

Survival, symptom onset, and rotarod studies. Mice were considered terminally paralyzed if they were unable to right themselves after 15 seconds of being placed on their backs. To assess symptom onset, mice were weighed daily, starting at 100 days of age. Weight data were then plotted to create a "weight curve." The peak of the weight curve was taken as the day of symptom onset. For the rotarod studies, mice were tested twice a week for 3 trials, each starting at 60 days of age, until they were unable to remain on the rotarod for at least 10 seconds. The best trial per day was recorded and used for analysis. Data were graphed as the percentage of the longest rotarod performance by each mouse.

Immunohistochemistry and antibodies. Spinal cords were fixed in 10% formalin for 24 hours and paraffin embedded. Six-μm sections were stained with the following antibodies: SOD1 (1:1,000; Calbiochem), activated caspase-3 (1:50; Cell Signaling Technology), choline acetyltransferase (1:25; Chemicon), LC3 (1:500; gift from J. Debnath, University of California, San Francisco), and p62 (1:250; Progen Biotechnik GmbH). Staining for activated caspase-3 was performed using the *PicTure*-MAX Polymer Detection Kit (Zymed Laboratories). TUNEL staining was performed using the ApopTag Peroxidase In Situ Apoptosis Detection Kit (Millipore). Activated caspase-3 and TUNEL stains were counterstained with cresyl violet. To quantify innervated neuromuscular junctions, medial gastrocnemii were fixed in 10% formalin for 24 hours, followed by 30% sucrose at 4°C for 24 hours. The samples were then embedded in OCT compound (Tissue-Tek) and flash frozen. Five-micron sections were fixed in acetone and stained with the following reagents: FITC-conjugated α-bungarotoxin (1:200; Sigma-Aldrich), anti-TUJ1 antibody (1:1,000; Covance), and Alexa Fluor 568–conjugated anti-mouse secondary antibody (1:1,000; Molecular Probes).

Motor neuron numbers were determined by staining lateral 6-μm sections of the lumbar spinal cord with cresyl violet. To determine the number of myelinated axons, sections of the lumbar ventral root were embedded in 1% agarose and fixed in Karnovsky's fixative (5% glutaraldehyde and 4% paraformaldehyde in 0.08 M sodium phosphate buffer) for at least 24 hours. The sections were then postfixed in osmium tetroxide and embedded in Epon. Sections were cut at 1 μm and stained with toluidine blue.

EM. Spinal cords were fixed in Karnovsky's fixative (5% glutaraldehyde and 4% paraformaldehyde in 0.08 M sodium phosphate buffer) for at least 24 hours and then treated with 2.5% glutaraldehyde in 0.1 M cacodylate buffer. The sections were then postfixed in osmium tetroxide and embedded in Epon. Sections were cut at 80 nm, stained with lead citrate and uranyl acetate, and examined under a Philips CM10 electron microscope.

Statistics. Kaplan-Meier survival curves were generated using Origin software and were analyzed using the log-rank test. Quantitative RT-PCR data, symptom onset, caspase-3 and TUNEL quantifications, innervated synapses, and motor neuron and myelinated axon numbers were compared using 2-tailed unpaired Student's t test. Rotarod data were compared using ANOVA. In figure legends, data are presented as mean ± SEM. P values of less than 0.05 were considered significant.

1. Bredesen DE. Programmed cell death mechanisms in neurological disease. *Curr Mol Med*. 2008;8(3):173–186.
2. Trushina E, McMurray CT. Oxidative stress and mitochondrial dysfunction in neurodegenerative diseases. *NeuroScience*. 2007;145(4):1233–1248.
3. Ellerby LM, et al. Kennedy's disease: caspase cleavage of the androgen receptor is a crucial event in cytotoxicity. *J Neurochem*. 1999;72(1):185–195.
4. Sathasivam S, Shaw PJ. Apoptosis in amyotrophic lateral sclerosis--what is the evidence? *Lancet Neurol*. 2005;4(8):500–509.
5. Tsai MS, Chiu YT, Wang SH, Hsieh-Li HM, Lian WC, Li H. Abolishing Bax-dependent apoptosis shows beneficial effects on spinal muscular atrophy model mice. *Mol Ther*. 2006;13(6):1149–1155.
6. Pasinelli P, Houseweart MK, Brown RH Jr, Cleveland DW. Caspase-1 and -3 are sequentially activated in motor neuron death in Cu,Zn superoxide dismutase-mediated familial amyotrophic lateral sclerosis. *Proc Natl Acad Sci U S A*. 2000;97(25):13901–13906.
7. Li M, et al. Functional role of caspase-1 and caspase-3 in an ALS transgenic mouse model. *Science*. 2000;288(5464):335–339.
8. Friedlander RM, Brown RH, Gagliardini V, Wang J, Yuan J. Inhibition of ICE slows ALS in mice. *Nature*. 1997;388(6637):31.
9. Ilangovan R, Marshall WL, Hua Y, Zhou J. Inhibition of apoptosis by Z-VAD-fmk in SMN-depleted S2 cells. *J Biol Chem*. 2003;278(33):30993–30999.
10. Ranganathan S, Harmison GG, Meyertholen K, Pennuto M, Burnett BG, Fischbeck KH. Mitochondrial abnormalities in spinal and bulbar muscular atrophy. *Hum Mol Genet*. 2009;18(1):27–42.
11. Palop JJ, Chin J, Mucke L. A network dysfunction perspective on neurodegenerative diseases. *Nature*. 2006;443(7113):768–773.
12. Stefani M. Generic cell dysfunction in neurodegenerative disorders: role of surfaces in early protein misfolding, aggregation, and aggregate cytotoxicity. *Neuroscientist*. 2007;13(5):519–531.
13. Lin MT, Beal MF. Mitochondrial dysfunction and oxidative stress in neurodegenerative diseases. *Nature*. 2006;443(7113):787–795.
14. Lindsten T, et al. The combined functions of pro-apoptotic Bcl-2 family members bak and bax are essential for normal development of multiple tissues. *Mol Cell*. 2000;6(6):1389–1399.
15. Wei MC, et al. Proapoptotic BAX and BAK: a requisite gateway to mitochondrial dysfunction and death. *Science*. 2001;292(5517):727–730.
16. Danial NN. BCL-2 family proteins: critical checkpoints of apoptotic cell death. *Clin Cancer Res*. 2007;13(24):7254–7263.
17. Green DR, Reed JC. Mitochondria and apoptosis. *Science*. 1998;281(5381):1309–1312.
18. Takeuchi O, Fisher J, Suh H, Harada H, Malynn BA, Korsmeyer SJ. Essential role of BAX,BAK in B cell homeostasis and prevention of autoimmune disease. *Proc Natl Acad Sci U S A*. 2005;102(32):11272–11277.
19. Tronche F, et al. Disruption of the glucocorticoid receptor gene in the nervous system results in reduced anxiety. *Nat Genet*. 1999;23(1):99–103.
20. Boillee S, et al. Onset and progression in inherited ALS determined by motor neurons and microglia. *Science*. 2006;312(5778):1389–1392.
21. Gurney ME, et al. Motor neuron degeneration in mice that express a human Cu,Zn superoxide dismutase mutation. *Science*. 1994;264(5166):1772–1775.
22. Gould TW, et al. Complete dissociation of motor neuron death from motor dysfunction by Bax deletion in a mouse model of ALS. *J Neurosci*. 2006; 26(34):8774–8786.
23. Liu J, Shinobu LA, Ward CM, Young D, Cleveland DW. Elevation of the Hsp70 chaperone does not effect toxicity in mouse models of familial amyotrophic lateral sclerosis. *J Neurochem*. 2005; 93(4):875–882.
24. Scott S, et al. Design, power, and interpretation of studies in the standard murine model of ALS. *Amyotroph Lateral Scler*. 2008;9(1):4–15.
25. Ruiz-Vela A, Opferman JT, Cheng EH, Korsmeyer SJ. Proapoptotic BAX and BAK control multiple initiator caspases. *EMBO Rep*. 2005;6(4):379–385.
26. Nishiyama J, Miura E, Mizushima N, Watanabe M, Yuzaki M. Aberrant membranes and double-membrane structures accumulate in the axons of Atg5-null Purkinje cells before neuronal death. *Autophagy*. 2007;3(6):591–596.
27. Kabeya Y, et al. LC3, a mammalian homologue of yeast Apg8p, is localized in autophagosome membranes after processing. *EMBO J*. 2000;19(21):5720–5728.
28. Bjorkoy G, et al. p62/SQSTM1 forms protein aggregates degraded by autophagy and has a protective effect on huntingtin-induced cell death. *J Cell Biol*. 2005;171(4):603–614.
29. Pankiv S, et al. p62/SQSTM1 binds directly to Atg8/LC3 to facilitate degradation of ubiquitinated protein aggregates by autophagy. *J Biol Chem*. 2007; 282(33):24131–24145.
30. Shimizu S, et al. Role of Bcl-2 family proteins in a non-apoptotic programmed cell death dependent on autophagy genes. *Nat Cell Biol*. 2004;6(12):1221–1228.
31. Arrasate M, Mitra S, Schweitzer ES, Segal MR, Finkbeiner S. Inclusion body formation reduces levels of mutant huntingtin and the risk of neuronal death. *Nature*. 2004;431(7010):805–810.
32. Lambert MP, et al. Diffusible, nonfibrillar ligands derived from Abeta1-42 are potent central nervous system neurotoxins. *Proc Natl Acad Sci U S A*. 1998;95(11):6448–6453.
33. Jyotika J, McCutcheon J, Laroche J, Blaustein JD, Forger NG. Deletion of the Bax gene disrupts sexual behavior and modestly impairs motor function in mice. *Dev Neurobiol*. 2007;67(11):1511–1519.
34. Kostic V, Jackson-Lewis V, de Bilbao F, Dubois-Dauphin M, Przedborski S. Bcl-2: prolonging life in a transgenic mouse model of familial amyotrophic lateral sclerosis. *Science*. 1997;277(5325):559–562.
35. Bassik MC, Scorrano L, Oakes SA, Pozzan T, Korsmeyer SJ. Phosphorylation of BCL-2 regulates ER Ca(2+) homeostasis and apoptosis. *EMBO J*. 2004; 23(5):1207–1216.
36. Pattingre S, et al. Bcl-2 antiapoptotic proteins inhibit Beclin 1-dependent autophagy. *Cell*. 2005; 122(6):927–939.
37. Vairo G, Innes KM, Adams JM. Bcl-2 has a cell cycle inhibitory function separable from its enhancement of cell survival. *Oncogene*. 1996;13(7):1511–1519.
38. Huang DC, O'Reilly LA, Strasser A, Cory S. The anti-apoptosis function of Bcl-2 can be genetically separated from its inhibitory effect on cell cycle entry. *EMBO J*. 1997;16(15):4628–4638.
39. Chauvier D, Ankri S, Charriaut-Marlangue C, Casimir R, Jacotot E. Broad-spectrum caspase inhibitors: from myth to reality? *Cell Death Differ*. 2007;14(2):387–391.
40. Soengas MS, et al. Apaf-1 and caspase-9 in p53-dependent apoptosis and tumor inhibition. *Science*. 1999;284(5411):156–159.
41. Ravikumar B, Rubinsztein DC. Can autophagy protect against neurodegeneration caused by aggregate-prone proteins? *Neuroreport*. 2004; 15(16):2443–2445.
42. Williams A, et al. Aggregate-prone proteins are cleared from the cytosol by autophagy: therapeutic implications. *Curr Top Dev Biol*. 2006;76:89–101.
43. Hara T, et al. Suppression of basal autophagy in neural cells causes neurodegenerative disease in mice. *Nature*. 2006;441(7095):885–889.
44. Komatsu M, et al. Loss of autophagy in the central nervous system causes neurodegeneration in mice. *Nature*. 2006;441(7095):880–884.
45. Hadano S, et al. Loss of ALS2/Alsin exacerbates motor dysfunction in a SOD1-expressing mouse ALS model by disturbing endolysosomal trafficking. *PLoS One*. 2010;5(3):e9805.
46. Hetz C, et al. XBP-1 deficiency in the nervous system protects against amyotrophic lateral sclerosis by increasing autophagy. *Genes Dev*. 2009; 23(19):2294–2306.
47. Gal J, et al. Sequestosome 1/p62 links familial ALS mutant SOD1 to LC3 via an ubiquitin-independent mechanism. *J Neurochem*. 2009;111(4):1062–1073.
48. Vila M, Przedborski S. Targeting programmed cell death in neurodegenerative diseases. *Nat Rev Neurosci*. 2003;4(5):365–375.